Empirical model for fusion cross sections of Ca-induced reactions

Reddi Rani. L[1] N. Sowmya[2†] K. N Sridhar[3] H C. Manjunatha[4‡] M. M. Armstrong Arasu[1]

[1]Department of Physics, St. Joseph's College (Autonomous), Affiliated to Bharathidasan University, Tiruchirappalli, 620002,TN, India
[2]Department of Physics,Govt.First.Grade College,Chikkaballapur- 562101, Karnataka,India
[3]Department of Physics,Govt.First.Grade College,Malur- 563160, Karnataka,India
[4]Department of Physics,Govt.First.Grade College,Devanahalli- 562110, Karnataka, India

Abstract: A new empirical formula for the astrophysical *S*-factor has been suggested as a function of the Coulomb interaction parameter, center of mass energy, and barrier height. About 22 fusion reactions with ^{40,48}Ca as projectiles were considered for different targets, leading to compound nuclei with atomic and mass numbers varying between $40 \le Z \le 112$ and $88 \le A \le 278$, respectively. The fusion cross-sections have been estimated using the geometric factor, the Gamow-Sommerfield factor, and the empirical formula for the *S*-factor. This study's findings showed better agreement with those of available experiments when compared to Wong's formula. The present work leads to a smaller standard deviation value than Wong's formula when used to correlate the experimental data of calcium-induced fusion reactions. Wong's formula provides a good approximation of fusion cross-sections when the center of mass energy is below the fusion barrier when compared to above the fusion barrier.

Keywords: fusion cross-sections, Wong formula, Gamow-Sommerfield-factor, Geometric-factor, *S*-factor

DOI: 10.1088/1674-1137/ad1a97

I. INTRODUCTION

In recent years, there has been a lot of interest in studying the effects of breakdown on fusion reactions in heavy-ion collisions at the Coulomb barrier [1–3]. The total fusion cross-section is the sum of complete fusion (CF) and incomplete complete fusion (ICF) cross-sections. ICF is the sum of sequential complete fusion (SCF) and direct complete fusion (DCF). If all the projectile fragments fuse with the target, then it is said to be SCF. DCF is the process by which a complete projectile fuses with the target without any breakup. From an experimental perspective, an SCF cannot be distinguished from a DCF.

Experimental measurements of ICF and CF cross sections are challenging. During the cooling process, the excited compound nucleus releases charged particles, which is especially important in light reaction systems. Only the TF cross-section may be measured since the residues from ICF and CF cannot be differentiated. The decay of the excited compound nucleus through the emission of charged particles can be insignificant in heavy reaction systems, allowing for independent CF cross-section measurements. Experimentally, CF cross-sections have been measured [4–9].

Earlier researchers [10] investigated heavy-ion fusion cross sections from ^{16}O+^{18}O to ^{64}Ni+^{124}Sn at extreme sub barrier energies with a simple formula. Umar *et al*. [11] uncovered evidence of the barrier's energy dependency by comparing fusion cross-sections estimated from potentials, *i.e.*, density-constrained n time-dependent Hartree-Fock approach obtained at different bombarding energies, with experimental data. The cold fusion reactions with $104 \le Z \le 112$ show larger fusion cross-sections below the bass barrier with 9−15 MeV of excitation energy [12, 13]. Rajbongshi *et al*. [14] investigated the role of the hexadecapole deformation effect of nuclei in the lanthanide region near the sub-barrier fusion cross-sections. Sub-barrier fusion reactions enhance the production cross-sections [15, 16].

Rowley and Hagino [17] examined the fusion cross sections of ^{l6}0+^{154}Sm and ^{12}C+^{12}C with generalized Wong and Hill-Wheeler formulae. Sedykh [18] proposed an empirical relation for the fusion cross-sections of heavy ions. Chushnyakova *et al*. [19] evaluated heavy ion fusion cross-sections with Hartree-Fock nuclear densities. Earlier studies show a detailed investigation of entrance channel parameters, deformation effect of projectile-target, optimal energy, possible projectile-target combinations, and rules for the selection of projectile-target combina-

Received 24 July 2023; Accepted 3 January 2024; Published online 4 January 2024
† E-mail: sowmyaprakash8@gmail.com
‡ E-mail: manjunathhc@rediffmail.com

tions [20–30]. The production cross section has been measured for the fusion reaction of the ^{16}O+^{27}Al system at different bombarding energies using the time-of-flight technique [31]. Fusion processes are distinguished by their fusion cross-sections, described by three energy-dependent functions: Gamow-Sommerfield, geometric, and astrophysical *S*-factors [32]. Hence, the main aim of the present work is to propose an empirical relation for the astrophysical *S*-factor for ^{40,48}Ca-induced fusion reactions. The fusion cross-sections obtained using three energy-dependent functions are compared with those of the available experimental data and fusion cross-sections obtained using Wong's formulae.

II. THEORETICAL FRAMEWORK

The fusion cross-section in terms of energy-dependent factors such as geometric, Gamow-Sommerfield, and astrophysical *S*-factor [33] is expressed as

$$\sigma_{\rm fus}(E) = \phi(E)G(E)S(E). \tag{1}$$

Here, the geometric factor ϕ term is inversely proportional to particle energy. $G(E)$ is the Gamow-Sommerfield factor, which is the penetration factor. Further, the *S*-factor, also known as the astrophysical *S*-factor, is a strong energy-correlated quantity dependent on the boundary conditions between the nuclear potential and the Coulomb electrostatic field.

A. Geometric-factor (ϕ)

In the majority of the fusion cross-section expressions, $\phi = \frac{1}{E}$. It is also denoted by the area occupied by a de-Broglie wavelength $\lambda\!\!\!^{-}$ or wavenumber k, which varies with energy and is expressed as

$$\phi(E) = \pi\lambda\!\!\!^{-2} = \frac{\pi}{k^2}, \tag{2}$$

where $k = \sqrt{2\mu E/\hbar}$ and $\mu = m_1m_2/(m_1+m_2)$ is the reduced mass of the system. The term $\phi(E)$ in terms of two independent terms is expressed as

$$\phi(E) = \pi\left(\frac{\hbar^2}{2\mu}\right)\frac{1}{E_{\rm cm}}. \tag{3}$$

B. Gamow-Sommerfield factor $G(E)$

The Gamow-Sommerfield factor $G(E)$ is a penetration factor of the Coulomb barrier by the incident particle that characterizes the likelihood of incident/target nuclei undergoing fusion. It is represented by an exponential attenuation function [34] expressed as

$$G(E) = \frac{1}{\chi^2} = \exp(-2\pi\eta_l), \tag{4}$$

the term η_l in the above equation is the Sommerfield parameter, and it is expressed as

$$\eta_l = \frac{1}{\pi}\int_{r_n}^{r_{\rm tp}} |k_l(r)|\,{\rm d}r, \tag{5}$$

where $k_l(r)$ is the wave number inside the nuclear well given by

$$k_l(r) = \left[\frac{2\mu}{\hbar^2}(E-U(r))\right]^{1/2}, \tag{6}$$

here, r_n and r_{tp} are the classical turning points. Under relativistic conditions, Eq. (4) [35] reduces as follows:

$$G(E) = \frac{2\pi}{\exp(2\pi/ka_c)-1}, \tag{7}$$

here, $a_c = \frac{\hbar^2}{k_eZ_1Z_2\mu e^2}$ with $k_e = \frac{1}{4\pi\epsilon_0}$

C. Astrophysical *S*-factor

The *S*-factor is a function that characterizes the width and energy of a nuclear reaction's resonance peaks. According to Miley *et al*. [32], the *S*-factor for light projectiles, such as T(d, n)^{4}He, ^{3}He(d, p)^{4}he, D(d, p)T, D(d, n)^{3}He, T(t, $2n$)^{4}He, T(^{3},X)Y^*, and ^{11}B(p, 2^4He)^{4}He is defined as follows:

$$S(E) = \frac{A_2}{(A_4-A_3E)^2+1} + A_5, \tag{8}$$

here, A_2, A_3, A_4. and A_5 are fitting constants [32]. However, in the present work, we have used experimental fusion cross-sections to evaluate the *S*-factor as follows;

$$S(E) = \frac{\sigma_{\rm fus}}{G\phi}, \tag{9}$$

here, $\sigma_{\rm fus}$ is the experimental fusion cross-section for ^{40,48}Ca-induced fusion reactions. Further, the *S*-factor is studied as a function of entrance channel parameters.

III. RESULTS AND DISCUSSIONS

In constructing the empirical formulae, we considered about 22 fusion reactions with ^{40,48}Ca as projectiles. These reactions are available in the existing literature [36–50]. The atomic and mass numbers of the com-

pound nuclei vary between $40 \le Z \le 112$ and $88 \le A \le 278$, respectively.

The fusion barrier heights of ^{40,48}Ca-induced fusion reactions are taken from nrv data [51]. Then, we plotted V_B as a function of $\frac{Z_1Z_2}{A_1^{1/3}+A_2^{1/3}}$, as represented in Fig. 1. The scatter symbol represents the fusion barrier height for ^{48}Ca-induced fusion reactions. The continuous line specifies the fitted equation for V_B as follows:

$$V_B = -7.62454 + 1.01166z + 4.92881\times10^{-4}z^2, \quad (10)$$

here, $Z = Z_1Z_2/(A_1^{1/3}+A_2^{1/3})$. The coefficient of determination is found to be $R^2 = 0.999$, and R^2 is explained in detail in the following paragraph. Hence, the target fusion barriers are evaluated most accurately by simply inputting the atomic and mass number of the projectile and target fusion barriers is evaluated most accurately. In all our further investigations, we considered the above empirical relation for V_B. As an illustration, we considered the fusion reaction of ^{40}Ca+^{46}Ti and plotted the astrophysical S-factor as a function of $E_{\rm cm}/V_B$ [47], as shown in Fig. 2. The value corresponding to the S-factor increases exponentially and reaches a maximum value as $E_{\rm cm}/V_B$ increases. Hence, we tried to fit a suitable equation, *i.e.*, a third-order polynomial equation fitted for S-factor values. The fitted equation as a function of $E_{\rm cm}/V_B$ is as follows;

$$S(E)^{PF} = B_0 + B_1\times\left(\frac{E_{\rm cm}}{V_B}\right) + B_2\times\left(\frac{E_{\rm cm}}{V_B}\right)^2 + B_3\times\left(\frac{E_{\rm cm}}{V_B}\right)^3, \quad (11)$$

here, B_0, B_1, B_2, and B_3 are the fitting constants. The hollow circle specifies the S-factor obtained using experimental fusion cross-sections, and the continuous red line corresponds to the fitted equation. The fitted equation is such that the coefficient of determination $R^2 \approx 1$. Where $R^2 = 1 - \frac{\sum_{i=1}^{n}(\hat{y}_i - y_i)^2}{\sum_{i=1}^{n}(y_i - \bar{y}_i)^2}$. Here, y_i is the S-factor obtained using experimental fusion cross-sections, $\bar{y}_i$ is the average value, and $\hat{y}_i$ is the value obtained from the present fitted equation. If the value of R^2 is close to one, it means that the value produced from the present fit is comparable to the value obtained for the S-factor using $\sigma_{\rm fus}$, Gamow-Sommerfield factor, and geometric factor. Accordingly, we obtained $R^2 = 0.9967$ for the fusion reaction of ^{40}Ca+^{46}Ti. Similarly, we explored all possible experimentally available ^{40,48}Ca-induced fusion reactions available in the literature.

Further, we emphasize the geometric factor, Gamow Sommerfield factor, S-factor, and fusion cross-sections as a function of $E_{\rm cm}$ for the fusion reaction of ^{40}Ca+^{46}Ti. Figure 3 (a)–(d) shows three dependent factors: ϕ, $G(E)$,

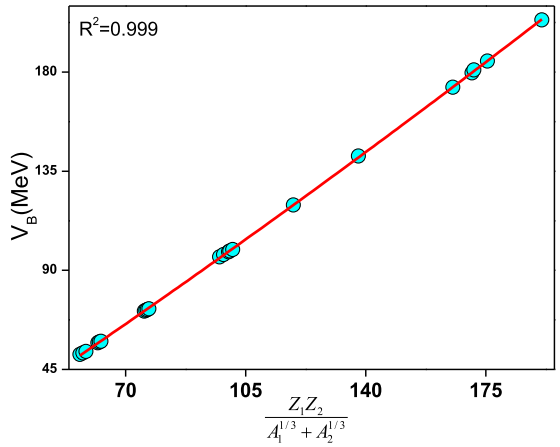

Fig. 1. (color online) A plot of fusion barrier (V_B) as function of the Coulomb interaction parameter.)

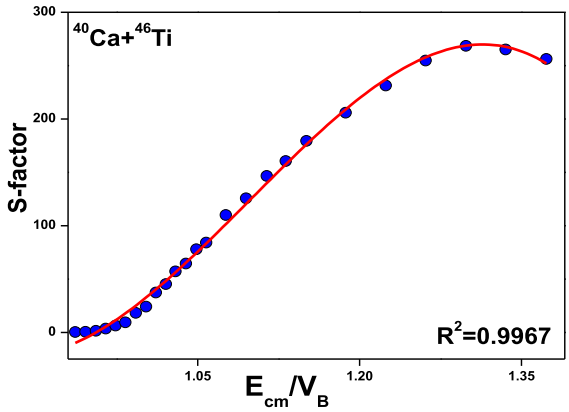

Fig. 2. (color online) A plot of the astrophysical S-factor as a function of $E_{\rm cm}/V_B$ for the fusion reaction of ^{40}Ca+^{46}Ti. The hollow circle specifies the S-factor obtained using experimental fusion cross-sections, and the continuous red line corresponds to the fitted equation.

and S-factor on the fusion cross-sections. Figure 3 (d) corresponds to the fusion cross-sections obtained using S-factor, $G(E)$, and ϕ as a function of $E_{\rm cm}$. From the figure, the ϕ noticeably decreases with an increase in $E_{\rm cm}$. Whereas, in the case of $G(E)$, the S-factor and $\sigma_{\rm fus}$ gradually increase with an increase in $E_{\rm cm}$. Further, we extended our studies to all ^{40,48}Ca-induced fusion reactions available in the literature [36–50]. Further, we gathered all fitting constants of ^{40,48}Ca-induced fusion reactions, and these fitting constants were again plotted as a function of different entrance channel parameters. The different entrance channel parameters [25]: mass asymmetry η_A, charge asymmetry α_Z, iso-spin asymmetry $\Delta(N/Z)$, charge product Z_1Z_2, Coulomb interaction parameter $(Z_1Z_2)/(A_1^{1/3}+A_2^{1/3})$, mean fissility χ_m and Z^2/A. The plot of B_0, B_1, B_2 and B_3, a function of the Coulomb interaction parameter (z), shows more systematic variation than

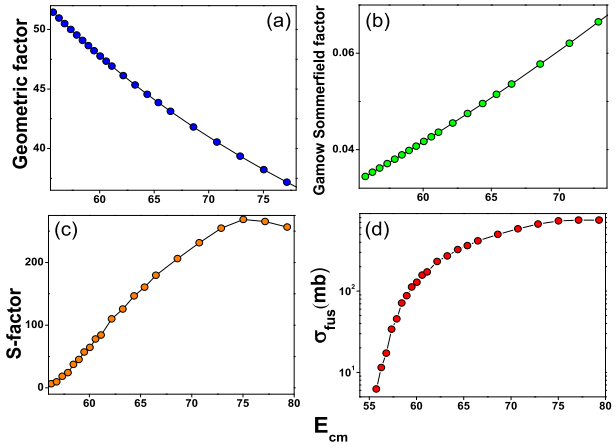

Fig. 3. (color online) (a) Geometric factor, (b) Gamow Sommerfield factor, (c) astrophysical *S*-factor, and (d) fusion cross-sections as a function of the center of mass-energy for the fusion reaction of ^{40}Ca+^{46}Ti.

all other studied entrance channel parameters. The best suitable fit corresponds to a fourth-order polynomial function. Consequently, we have fitted an empirical relation for B_0, B_1, B_2, and B_3 as a function of the Coulomb interaction parameter, and it is given by

$$B_0=\sum_{i=0}^{4}B_{i0}z^i,\quad B_1=\sum_{i=0}^{4}B_{i1}z^i,$$
$$B_2=\sum_{i=0}^{4}B_{i2}z^i,\quad B_3=\sum_{i=0}^{4}B_{i3}z^i, \tag{12}$$

here, B_{i0}, B_{i1}, B_{i2}, and B_{i3} are the fitting constants whose values are tabulated in Table 1.

With the benefit of the empirical formula for the *S*-factor and derived fusion barrier height, we extend our studies to reproduce experimental fusion cross-sections. Hence, the fusion cross-section expression is as follows:

$$\sigma_{\rm fus}=\frac{2\pi^2\hbar^2}{2\mu E_{\rm cm}(\exp(2\pi/ka_c)-1)}\left[B_0+B_1\times\left(\frac{E_{\rm cm}}{V_B}\right)+B_2\times\left(\frac{E_{\rm cm}}{V_B}\right)^2+B_3\times\left(\frac{E_{\rm cm}}{V_B}\right)^3\right]. \tag{13}$$

Figure 4 (a)−(f) shows a comparison between fusion cross-sections obtained from the present work and Wong's formula with that of experimental fusion cross-sections for ^{40,48}Ca-induced fusion reactions. In the case of Wong's formula [52, 53] the fusion cross-sections are

Table 1. Tabulation of fitting constants for different Coulomb interaction regions.

Parameters	Coulomb interaction regions				
	$56.70 \le z \le 62.37$	$62.83 \le z \le 76.80$	$97.40 \le z \le 101.24$	$118.95 \le z \le 165.41$	$169.40 \le z \le 191.32$
$\mathbf{B_{00}}$	−28332537697.0978	−64435938215.0135	2203255720.78296	−656384034.537705	718103288.995812
$\mathbf{B_{10}}$	1899266991.06486	3565880041.22783	−89697465.9448795	18672321.6099274	−16198443.3275908
$\mathbf{B_{20}}$	−47716329.8469277	−73813845.3711374	1369263.5571222	−198214.503445243	136937.60578956
$\mathbf{B_{30}}$	532495.452482732	677530.491177697	−9289.07320486588	930.717074241155	−514.173351049124
$\mathbf{B_{40}}$	−2227.14309130892	−2327.24022733404	23.6292964092531	−1.63119412248294	0.723493714869457
$\mathbf{B_{01}}$	74155501865.1684	179936541485.059	−8062716463.75572	1013137999.93127	−2274900515.76646
$\mathbf{B_{11}}$	−4969960187.56886	−9957975694.56154	327450781.216016	−28819904.5885794	51341614.3086018
$\mathbf{B_{21}}$	124836976.199133	206136910.648799	−4986709.86432899	305920.755546077	−434246.147680954
$\mathbf{B_{31}}$	−1392842.15972741	−1892172.76748474	33749.8813175876	−1436.37270074054	1631.30728770228
$\mathbf{B_{41}}$	5824.31016914153	6499.61337173533	−85.6514768172259	2.51726251217576	−2.29651664486989
$\mathbf{B_{02}}$	−64538359422.0306	−166944972987.738	9503015946.60498	−521686292.017596	2360492170.49599
$\mathbf{B_{12}}$	4324462380.47212	9239263377.64448	−385301520.830439	14839439.5263792	−53294534.9065123
$\mathbf{B_{22}}$	−108599446.500798	−191264697.071673	5857989.12492678	−157510.753257383	450940.31810073
$\mathbf{B_{32}}$	1211412.51240851	1755710.90176198	−39581.4376985516	739.500655641065	−1694.67147551589
$\mathbf{B_{42}}$	−5064.55339797348	−6031.05442556466	100.286858383963	−1.29588145351538	2.38661560001902
$\mathbf{B_{03}}$	18836106053.3082	51455405399.732	−3630526068.45853	89644054.0631107	−806569328.034477
$\mathbf{B_{13}}$	−1261880703.88212	−2847777630.14262	147025738.783876	−2549897.67189143	18216456.6717986
$\mathbf{B_{23}}$	31683084.9748326	58954239.6708472	−2232687.02980118	27064.1525036251	−154184.167008323
$\mathbf{B_{33}}$	−353351.05279423	−541184.190230803	15068.1373241659	−127.05460664328	579.619434940112
$\mathbf{B_{43}}$	1476.96725249418	1859.07766520354	−38.1331586988069	0.222625894265698	−0.816532819909371

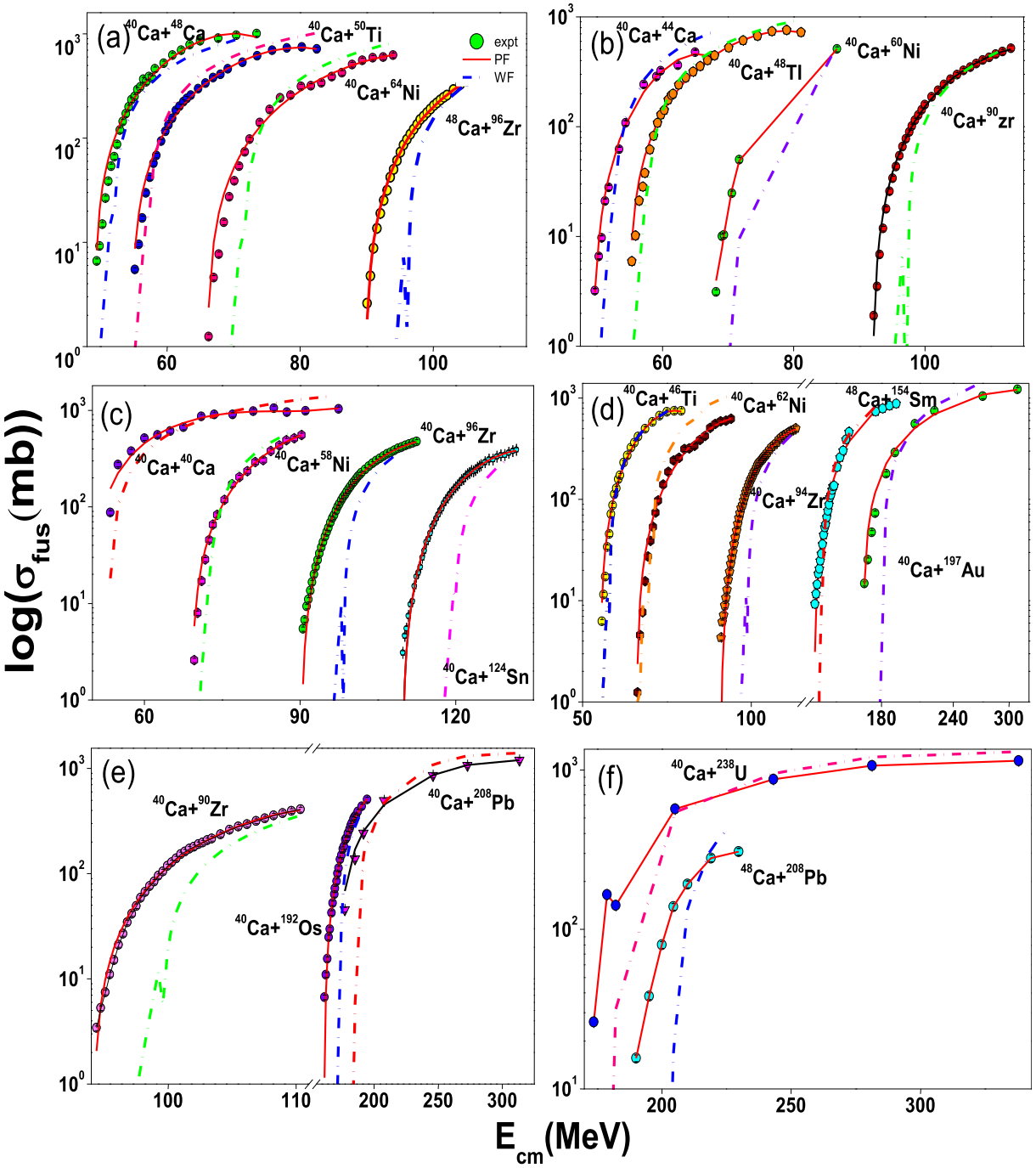

Fig. 4. (color online) Comparison of fusion cross-sections obtained from the present work with those of the experimental fusion cross-sections and those obtained using Wong's formula for ^{40,48}Ca-induced fusion reactions. Here, the scatter symbol specifies the experimental data. The continuous and dash-dot lines correspond to the fusion cross-sections obtained in the present work and using Wong's formula, respectively.

evaluated as follows:

$$\sigma_{\rm fus}^{\rm Wong}=\begin{cases}\dfrac{R_B^2\hbar\omega}{2E_{\rm cm}}\ln\left[1+\exp\left(\dfrac{2\pi}{\hbar\omega}{\rm cm}-V_B\right)\right], & E_{\rm cm}\le V_B\\ \pi R_B^2\left(1-\dfrac{V_B}{E_{\rm cm}}\right), & E_{\rm cm}\ge V_B\end{cases} \tag{14}$$

here, $\hbar\omega$, R_B, and V_B are the inverted parabola, fusion barrier height, and barrier position. Further, a close examination of Fig. 4 (a) reveals that the fusion cross-sections obtained from the present work are in good agreement with those of available experimental values when compared to the fusion cross-sections estimated from the Wong formula. In all the studied fusion reactions, the

cross-sections noticeably increase with an increase in $E_{\rm cm}$. Further, the fusion cross-sections produced by the Wong formula below the fusion barrier are in good agreement with that of the experimental data. However, a larger deviation from the experimental value is observed when $E_{\rm cm}$ is above the fusion barrier. Hence, Wong's formula reproduces the experimental fusion cross-sections with less deviation when $E_{\rm cm}$ is below the fusion barrier compared to the above fusion barrier for the ^{40,48}Ca-induced fusion reactions.

Further, to check the applicability of the proposed empirical formula, the present formula is applied for fusion reactions, which were not considered when constructing the formula. To illustrate, we reproduced fusion cross-sections for the ^{48}Ca+^{194}Pt reaction and compared them with those of the experiments and Wong's formalism. The values produced by the present formula are close to those of the experiments when compared to Wong's formula, as shown in Fig. 5. Furthermore, we used the standard deviation as a goodness of fit measure. It defines how well the value obtained from the present fit agrees with the experimental data. The standard deviation is evaluated as follows:

$$\sigma = \sqrt{\frac{1}{N-1}\sum_{i=1}^{n}(O_i - E_i)^2}. \tag{15}$$

Here, O_i is the observed value obtained from the present fit, and E_i is the experimental value. N is the total number of values considered in each fusion reaction. The standard deviation obtained using the present work and Wong's formula is also tabulated in Table 2. From the table, the standard deviation obtained using the present work is found to be smaller than that of Wong's formula for ^{40,48}Ca-induced fusion reactions. Consequently, more accurate and exact fusion cross-sections may be predicted using the geometric factor, Gamow-Sommerfield factor, and empirical formula of the S-factor for ^{40,48}Ca-induced fusion cross-sections.

IV. Conclusions

In the present study, we investigated ^{40,48}Ca-induced fusion cross-sections. The empirical formulae for the astrophysical S-factor are deduced using experimental fusion cross-sections, Gammow-factor (ϕ), and Gammow-Sommerfield factor $G(E)$. Further, the fitting constants for each fusion reaction are made independent using the effect of entrance channel parameters. Accordingly, the S-factor reproduces experimental fusion cross-sections more accurately and precisely when compared to Wong's formula for ^{40,48}Ca-induced fusion reactions. The present study contributes to predicting the fusion cross-sections for ^{40,48}Ca-induced reactions leading to compound nuclei with atomic and mass numbers varying between $40 \le Z \le 112$ and $88 \le A \le 278$ respectively.

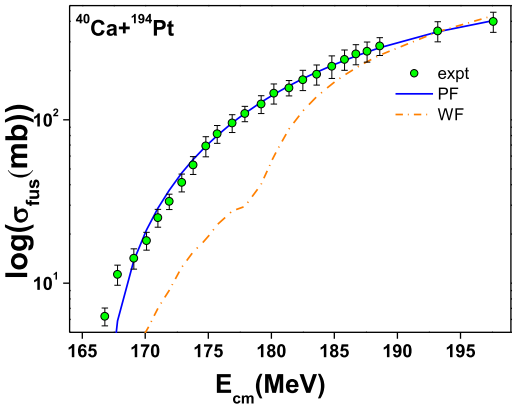

Fig. 5. (color online) A comparison of the fusion cross-sections obtained using the present formula with those of the available experiment [54] and Wong's formula.

Table 2. Tabulation of the standard deviations obtained from the present formula ($\sigma_{\rm fus}^{PF}$) and Wong's formula ($\sigma_{\rm fus}^{\rm Wong}$) with those of available experimental values. We also tabulated the range of $E_{\rm cm}$ considered in predicting the fusion cross-sections.

Reaction	Range of $E_{\rm cm}$ /MeV	$\sigma_{\rm fus}^{PF}$	$\sigma_{\rm fus}^{\rm Wong}$
^{40}Ca+^{48}Ca	90.71-134.8	29.04	318.47
^{40}Ca+^{44}Ca	49.75-67.6	17.99	107.24
^{40}Ca+^{40}Ca	53.46-97.46	41.94	187.05
^{40}Ca+^{50}Ti	55.23-82.55	2.17	22.41
^{40}Ca+^{48}Ti	55.37-81.13	2.18	13.75
^{40}Ca+^{46}Ti	55.76-79.34	2.22	7.45
^{40}Ca+^{64}Ni	66.29-93.99	4.14	21.62
^{40}Ca+^{62}Ni	70-106.7	7.34	18.35
^{40}Ca+^{60}Ni	68.2-86.6	0.62	13.97
^{40}Ca+^{58}Ni	69.64-90.34	2.46	15.26
^{48}Ca+^{96}Zr	90.1-112.1	3.06	46.18
^{48}Ca+^{90}Zr	92.2-113.1	4.61	37.82
^{40}Ca+^{96}Zr	128.36-159.38	2.67	72.97
^{40}Ca+^{94}Zr	91.124-113.22	3.86	74.46
^{40}Ca+^{90}Zr	136.37-159.38	0.69	11.66
^{40}Ca+^{124}Sn	109.82-131.75	3.68	92.33
^{48}Ca+^{154}Sm	138.01-191.12	26.91	72.83
^{40}Ca+^{192}Os	161.2-194.5	5.31	76.97
^{40}Ca+^{197}Au	168.16-310.71	38.70	250.22
^{48}Ca+^{208}Pb	173.71-338.08	30.50	495.49
^{40}Ca+^{208}Pb	177.14-313.51	24.22	305.80
^{40}Ca+^{238}U	190.1-229.8	5.31	109.32

References

[1] L. Canto, P. Gomes, R. Donangelo *et al.*, Phys. Rep. **424**, 1 (2006)
[2] N. Keeley, R. Raabe, N. Alamanos *et al.*, Progress in Particle and Nuclear Physics **59**, 579 (2007)
[3] B. Back, H. Esbensen, C. Jiang *et al.*, Rev. Mod. Phys. **86**, 317 (2014)
[4] K. Kalita, Journal of Physics G: Nuclear and Particle Physics **38**, 095104 (2011)
[5] L. Gasques, D. Hinde, M. Dasgupta *et al.*, Phys. Rev. C **79**, 034605 (2009)
[6] V. Tripathi, A. Navin, V. Nanal *et al.*, Phys. Rev. C **72**, 017601 (2005)
[7] P. Rath, S. Santra, N. Singh *et al.*, Phys. Rev. C **79**, 051601 (2009)
[8] Z. Liu, C. Signorini, M. Mazzocco *et al.*, Eur. Phys. J. A **26**, 73 (2005)
[9] A. Shrivastava, A. Navin, A. Lemasson *et al.*, Phys. Rev. Lett. **103**, 232702 (2009)
[10] C. Jiang, K. Rehm, B. Back *et al.*, Eur. Phys. J. A **54**, 1 (2018)
[11] A. Umar, C. Simenel, and V. Oberacker, Phys. Rev. C **89**, 034611 (2014)
[12] S. Hofmann, V. Ninov, F. Heßberger *et al.*, Zeitschrift für Physik A Hadrons and Nuclei **350**, 277 (1995)
[13] S. Hofmann, V. Ninov, F. Hessberger *et al.*, Zeitschrift für Physik A Hadrons and Nuclei **354**, 229 (1996)
[14] T. Rajbongshi, K. Kalita, S. Nath *et al.*, Phys. Rev. C **93**, 054622 (2016)
[15] V. Parkar, R. Palit, S. K. Sharma *et al.*, Phys. Rev. C **82**, 054601 (2010)
[16] K. Rehm, H. Esbensen, C. Jiang *et al.*, Phys. Rev. Lett. **81**, 3341 (1998)
[17] N. Rowley and K. Hagino, Phys. Rev. C **91**, 044617 (2015)
[18] V. Y. Denisov and I. Y. Sedykh, The Eur. Phys. J. A **55**, 153 (2019)
[19] M. Chushnyakova, R. Bhattacharya, and I. Gontchar, Phys. Rev. C **90**, 017603 (2014)
[20] H. C. Manjunatha, Y. S. Vidya, P. S. D. Gupta *et al.*, Journal of Physics G: Nuclear and Particle Physics **49**, 125101 (2022)
[21] H. C. Manjunatha, P. S. D. Gupta, N. Sowmya *et al.*, Phys. Rev. C **104**, 024622 (2021)
[22] P. S. D. Gupta, N. Sowmya, H. C. Manjunatha *et al.*, Phys. Rev. C **106**, 064603 (2022)
[23] H. C. Manjunatha, P. S. Damodara Gupta, N. Sowmya *et al.*, Int. J. Mod. Phys. E **31**, 2250015 (2022)
[24] P. S. D. Gupta, H. C. Manjunatha, and N. Sowmya, Braz. J. Phys. **51**, 1803 (2021)
[25] H. C. Manjunatha, N. Sowmya, N. Manjunatha *et al.*, Phys. Rev. C **102**, 064605 (2020)
[26] N. Sowmya and H. C. Manjunatha, Braz. J. Phys. **49**, 874 (2019)
[27] H. C. Manjunatha, K. N. Sridhar, and N. Sowmya, Phys. Rev. C **98**, 024308 (2018)
[28] H. Manjunatha, K. Sridhar, and N. Sowmya, Nucl. Phys. A **987**, 382 (2019)
[29] H. C. Manjunatha, L. Seenappa, N. Sowmya *et al.*, Can. J. Phys. **99**, 16 (2021)
[30] P. S. D. Gupta, H. C. Manjunatha, N. Sowmya *et al.*, Pramana **96**, 146 (2022)
[31] B. Back, R. Betts, C. Gaarde *et al.*, Nucl. Phys. A **285**, 317 (1977)
[32] G. Miley, H. Towner, and N. Ivich, *Fusion Cross Sections and Reactivities (Univ. of Illinois) Rep*, Tech. Rep. (COO-2218-17, 1974)
[33] X. Z. Li, Fusion science and technology **41**, 63 (2002)
[34] J. Brennan and J. Coyne, Journal of Research of the National Bureau of Standards **68**, 675 (1964)
[35] X. Z. Li, B. Liu, Q. M. Wei *et al.*, Fusion engineering and design **81**, 1517 (2006)
[36] M. Trotta, A. Stefanini, L. Corradi *et al.*, Phys. Rev. C **65**, 011601(R) (2001)
[37] H. Aljuwair, R. Ledoux, M. Beckerman *et al.*, Phys. Rev. C **30**, 1223 (1984)
[38] H. Doubre, A. Gamp, J. Jacmart *et al.*, Phys. Lett. B **73**, 135 (1978)
[39] A. A. Sonzogni, J. Bierman, M. Kelly *et al.*, Phys. Rev. C **57**, 722 (1998)
[40] B. Sikora, J. Bisplinghoff, W. Scobel *et al.*, Phys. Rev. C **20**, 2219 (1979)
[41] A. Stefanini, F. Scarlassara, S. Beghini *et al.*, Phys. Rev. C **73**, 034606 (2006)
[42] H. Timmers, D. Ackermann, S. Beghini *et al.*, Nucl. Phys. A **633**, 421 (1998)
[43] A. Stefanini, B. Behera, S. Beghini *et al.*, Phys. Rev. C **76**, 014610 (2007)
[44] F. Scarlassara, S. Beghini, G. Montagnoli *et al.*, Nucl. Phys. A **672**, 99 (2000)
[45] M. Trotta, A. Stefanini, S. Beghini *et al.*, Eur. Phys. J. A **25**, 615 (2005)
[46] R. Sagaidak, G. Kniajeva, I. Itkis *et al.*, Phys. Rev. C **68**, 014603 (2003)
[47] R. Vandenbosch, A. Sonzogni, and J. Bierman, Journal of Physics G: Nuclear and Particle Physics **23**, 1303 (1997)
[48] J. Bierman, P. Chan, J. Liang *et al*, Phys. Rev. Letters **76**, 1587 (1996)
[49] A. Pacheco, J. F. Niello, D. DiGregorio *et al.*, Phys. Rev. C **45**, 2861 (1992)
[50] K. Nishio, S. Mitsuoka, I. Nishinaka *et al.*, Phys. Rev. C **86**, 034608 (2012)
[51] Nrv video project, http://nrv.jinr.ru/nrv/webnrv/fusion/reactions.html.
[52] C. Wong, Phys. Rev. Lett. **31**, 766 (1973)
[53] H. Manjunatha and K. Sridhar, BRr **2**, 2 (2016)
[54] J. Bierman, P. Chan, J. Liang *et al.*, Phys. Rev. C **54**, 3068 (1996)